# Optical modulation and detection in slotted Silicon waveguides

**T. Baehr-Jones and M. Hochberg**

*Department of Applied Physics, California Institute of Technology, 1200 E California Blvd., Pasadena CA 91125*
*thorolf@caltech.edu, hochberg@caltech.edu*

**Guangxi Wang**

*Department of Electrical Engineering, California Institute of Technology, 1200 E California Blvd., Pasadena CA 91125*

**R. Lawson, Y. Liao, P. A. Sullivan, and L. Dalton**

*Department of Chemistry, University of Washington, Seattle, Washington, 98195*

**A. K.-Y. Jen**

*Department of Materials Science and Engineering, University of Washington, Seattle, Washington, 98195*

**A. Scherer**

*Department of Applied Physics, California Institute of Technology, 1200 E California Blvd., Pasadena CA 91125*

**Abstract**: We demonstrate a novel mechanism for low power optical detection and modulation in a slotted waveguide geometry filled with nonlinear electro-optic polymers. The nanoscale confinement of the optical mode, combined with its close proximity to electrical contacts, enables the direct conversion of optical energy to electrical energy, without external bias, via optical rectification, and also enhances electro-optic modulation. We demonstrate this process for power levels in the sub-milliwatt regime, as compared to the kilowatt regime in which optical nonlinear effects are typically observed at short length scales. Our results suggest that a new class of detectors based on nonlinear optics may be practical.



**OCIS Codes:** (040.0040) Detectors, (040.6040) Silicon, (060.4080) Modulation, (130.0130) Integrated Optics, (130.2790) Guided Waves, (130.3120) Integrated Optics Devices, (130.4310) Nonlinear, (160.5470) Polymers, (190.0190) Nonlinear Optics, (230.0040) Detectors, (230.4110) Modulators

## References and links

1. R. A. Soref, J. P. Lorenzo, "All-Silicon Active and Passive Guided-Wave Components For Lambda=1.3 and 1.6 MU-M," IEEE J. Quantum Electron. **22**, 873-879 (1986).
2. A. S. Liu, R. Jones, L. Liao, D. Samara-Rubio, D. Rubin, O. Cohen, R. Nicolaescu, M. Paniccia, "A high-speed silicon optical modulator based on a metal-oxide-semiconductor capacitor," Nature **427**, 615-618 (2004)
3. A. Scherer, O. Painter, J. Vuckovic, M. Loncar, T. Yoshie, "Photonic crystals for confining, guiding and emitting light," IEEE T. Nanotechnol. **1**, 4-11 (2002).
4. A. Layadi, A. Vonsovici, R. Orobtchouk, D. Pascal, A. Koster, "Low-loss optical waveguide on standard SOI/SIMOX substrate," Opt. Commun **146**, 31-33 (1998).
5. Q. F. Xu, V. R. Almeida, R. R. Panepucci, M. Lipson, "Guiding and Confining Light in Void Nanostructures," Opt. Lett. **29**, 1206-1211 (2004).
6. T. Baehr-Jones, M. Hochberg, C. Walker, A. Scherer, "High-Q optical resonators in silicon-on-insulator-based slot waveguides," Appl. Phys. Lett. **86**, 081101 (2005).
7. M. Bass, P. A. Franken, J. F. Ward, G. Weinreich, "Optical Rectification," Phys. Rev. Lett. 9, 446 (1962).
8. L. R. Dalton, "Organic electro-optic materials," Pure Appl. Chem. **76**, 1421-1433 (2004).

#7444 - $15.00 USD Received 16 May, 2005; revised 20 June, 2005; accepted 23 June, 2005

9. Y. Y. Huang, G. T. Paloczi, A. Yariv, C. Zhang, L. R. Dalton, "Fabrication and replication of polymer integrated optical devices using electron-beam lithography and soft lithography," J. Phys. Chem. B. **108**, 8606-8613 (2004).
10. A. Nahata, D. H. Auston, C. J. Wu, J. T. Yardley, "Generation of Terahertz Radiation From a Poled polymer," Appl. Phys. Lett., **67**, 1358-1360 (1995).
11. F. Pockels, Lehrbuch der Kristalloptik (B. G. Teubner, Leipzig and Berlin, 1906).
12. C. Zhang, L. R. Dalton, M. C. Oh, H. Zhang, W. H. Steier, " Low V-pi electrooptic modulators from CLD-1: Chromophore design and synthesis, material processing, and characterization," Chem. Mater. **13**, 3043-3050 (2001).
13. Silicon Genesis Corporation, 61 Daggett Drive, San Jose, CA 95134.
14. Dendrimer Material results are currently in preparation
15. A. Taflove, *Computational Electrodynamics*, (Artech House, Boston, MA, 1995).
16. D. Taillaert, P. Bienstman, R. Baets, "Compact efficient broadband grating coupler for silicon-on-insulator waveguides," Opt. Lett. **29**, 2749-2751 (2004).
17. R. Boyd, *Nonlinear Optics*, Second Edition (Academic Press, New York, 2003).
18. S. Graf, H. Sigg, W. Bachtold, "High-frequency electrical pulse generation using optical rectification in bulk GaAs," Appl. Phys. Lett. **76,** 2647-2649 (2000).

## 1. Introduction

Waveguide-based integrated optics in silicon [1] provides an ideal platform for concentrating and guiding light at the nanoscale. The high index contrast between silicon and common cladding materials enables extremely compact waveguides with very high mode field concentrations, and allows the use of established CMOS fabrication techniques to define photonic integrated circuits [2-4]. It has recently become possible, by using slotted waveguides [5], to further concentrate a large fraction of the guided mode into a gap within the center of a silicon waveguide. This geometry greatly magnifies the electric field associated with the optical mode, resulting in electric fields in excess of $10^6$ V/m for continuous-wave, sub-millitwatt optical signals. Moreover, since the slotted geometry consists of two silicon strips which can be electrically isolated, a convenient mechanism for electro-optic interaction is provided. Such waveguides can be fabricated with low loss; we have previously demonstrated -10dB/cm [6].

Here we exploit both the high intensity of the optical field and the close proximity of the electrodes for several purposes. First, and perhaps most significantly, we demonstrate detection of optical signals via direct conversion to electrical energy by means of nonlinear optical rectification [7]. Our device consists of a ring resonator with an electro-optic polymer based $\chi^2$ material deposited as a cladding [8, 9]. Inside the slot, the high optical field intensity creates a standing DC field, which creates a virtual voltage source between the two silicon electrodes, resulting in a measurable current flow, in the absence of any external electrical bias. Though optical rectification has been observed in electro-optic polymers elsewhere [10], typically instantaneous optical powers on the order of 1 kW are needed for observable conversion efficiencies, often achieved with pulsed lasers. We demonstrate measurable conversion with less than 1 mW of non-pulsed input, obtained from a standard, low power tunable laser near 1500 nm.

We also demonstrate standard Pockels' effect based modulation [11], which is similarly enhanced by means of the very small scale of our device. The close proximity of the electrodes, and ready overlap with the optical mode, causes an external voltage to produce a far larger effective electric modulation field, and therefore refractive index shift, than would be obtained through conventional waveguide designs [12]. We demonstrate this through the tuning of the resonance frequencies of a slot waveguide ring resonator.

## 2. Device fabrication

### *2.1 Waveguide fabrication*

The devices described in this paper were fabricated in electronic grade silicon-on-insulator (SOI) [13] with a top layer thickness of 110 nm and an oxide thickness of 1.3 microns. The silicon layer is subsequently doped to approximately $10^{19}$ Phosphorous atoms/cm$^3$, yielding

#7444 - $15.00 USD Received 16 May, 2005; revised 20 June, 2005; accepted 23 June, 2005

resistivities after dopant activation of ~0.025 ohm-cm. EO polymers were then spin-deposited onto the waveguide structures and subsequently poled by using a high field applied across the slot in the waveguide

Lithography was performed using a Leica EBPG 5000+ electron beam system at 100kv. Prior to lithography, the samples were manually cleaved, cleaned in acetone and isopropanol, baked for 20 minutes at 180C, coated with 2 percent HSQ resist from Dow Corning Corporation, spun for two minutes at 1000 rpm, and baked for an additional 20 minutes. The samples were exposed at 5 nm step size, at 3500 $\mu C/cm^2$. The samples were developed in AZ 300 TMAH developer for 3 minutes, and etched on an Oxford Instruments PLC Plasmalab 100 with chlorine at 80 sccm, forward power at 50 W, ICP power at 800 W, 12 mTorr pressure, and 33 seconds of etch time. The samples were then implanted with phosphorous at normal incidence, 30keV energy, and $1x10^{14}$ ions/$cm^2$ density. The sample was annealed under a vacuum at 950C in a Jipilec Jetstar rapid thermal annealer, and the samples were dipped in buffered hydrofluoric in order to remove the remnants of electron beam resist from the surface.

After initial optical testing, the samples were coated with YLD 124 electrooptic polymer, and in one case with dendrimer-based electrooptic material [14]. The samples were stored under a vacuum at all times when they were not being tested, in order to reduce the chances of any degradation.

*2.2 Synthesis of YLD 124 coating solution*

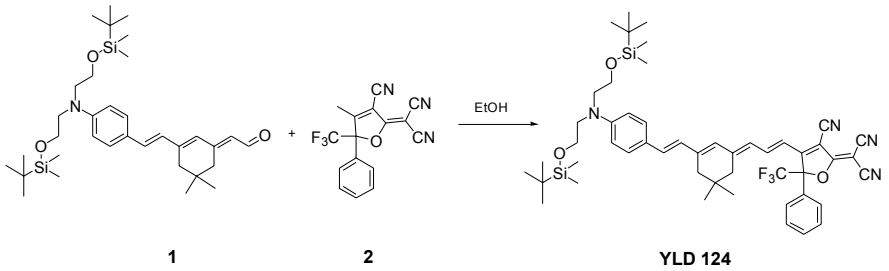


Fig. 1. Synthesis of YLD 124.

To a solution of 0.56 g (0.96 mmol) of 1 [12] and 0.36 g of 2 (1.1 mmol) in 1.5 mL of THF was added 6 mL of absolute ethanol. The mixture was stirred for 6 h at room temperature. The precipitate was collected by filtration and washed by ethanol and methanol. The crude product was dissolved in minimum amount of $CH_2Cl_2$. The resultant solution was added dropwisely to 100 mL of methanol. The product (0.76 g) was collected as dark green precipitate. Yield was 90%. $^1$H NMR ($CDCl_3$): 8.05 (t, J=13.6 Hz, 1H ), 7.45-7.58 (m, 5 H), 7.38 (d, J=8.9 Hz, 2H) 6.93 (d, J=15.9 Hz, 1 H) 6.79 (d, J=15.9 Hz, 1H), 6.70 (d, J=8.9 Hz, 2H), 6.40-6.25 (m, 3 H), 3.80 (t, J=5.8 Hz, 4H), 3.59 (t, J=5.8 Hz, 4H), 2.42 (s, 2H), 2.40 (s, 2H), 1.04 (s, 3H), 0.98 (s, 3H), 0.90 (s, 18H), 0.04 (S, 12H). MS (ESP): 879.48 (M+H). UV-Vis (THF): 765 nm. m.p. 173 $^o$C

One part of YLD124 was mixed with three parts of APC (Poly[Bisphenol A carbonate-co-4,4'-(3,3,5-trimethylcyclohexylidene)diphenol carbonate]). The mixture was dissolved in cyclopentanone. The total solid content (YLD124 and APC) is about 12%. The resultant solution was filtered through a 0.2 μm filter before used on device.

## 3. Results

*3.1 Optical rectification based detection*

#7444 - $15.00 USD Received 16 May, 2005; revised 20 June, 2005; accepted 23 June, 2005

Figure 2 details the complete geometry of the photodetectors and filters, including a cross section of the slotted waveguide. In Fig. 2(a), the optical mode was solved using a finite-difference based Hermetian Eigensolver [15], and has an effective index of approximately 1.85 at 1500nm. Most of the electric field is parallel to the plane of the chip, and it is possible to contact both sides of the slot in a slotted ring resonator, as shown in Fig. 2(b). Electrically isolated contacts between the silicon rails defining the slotted waveguide introduce only about 0.1 dB of optical loss. Figure 2(c) details the layout of a complete slotted ring resonator, with two contact pads connected to the outer half of the ring, and two pads electrically connected to the inner half of the ring. A shunt resistor provides a means of confirming electrical contact, and typical pad-to-pad and pad-to-ring resistances range from 1MΩ to 5 MΩ. Figure 2(d) displays a typical electrically contacted slotted ring described in this study.

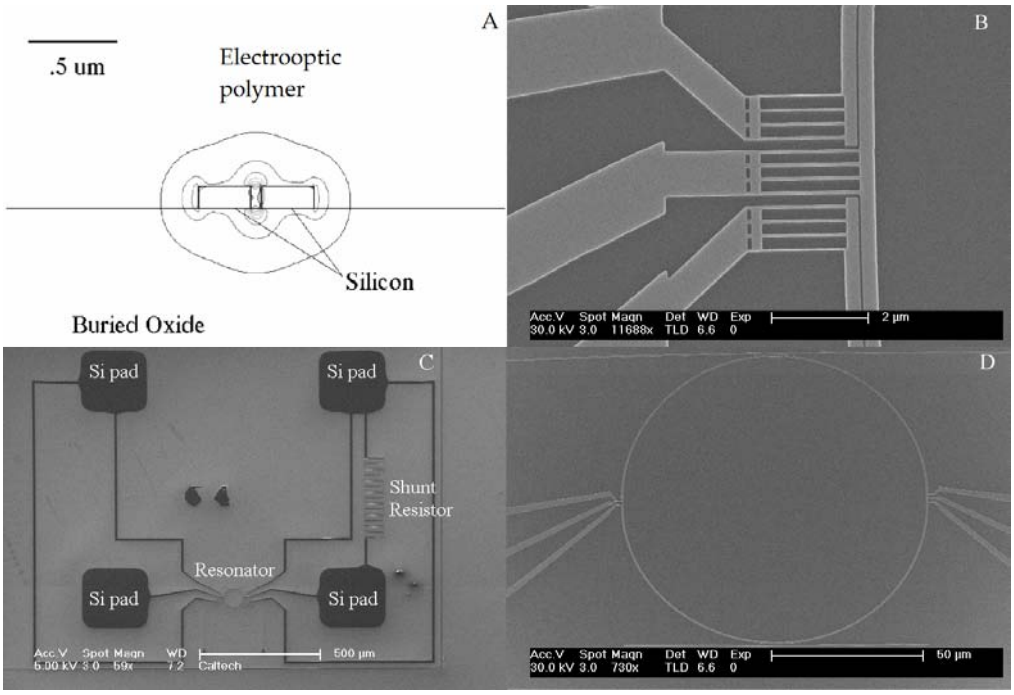


Fig. 2. Panel A shows a cross section of the geometry with optical mode superimposed on a waveguide. Panel B shows a SEM image of the resonator electrical contacts. Panel C shows the logical layout of device, superimposed on a SEM image. Panel D is an image of the ring and the electrical contact structures.

Testing was performed with single-mode polarization maintaining input and output fibers, grating coupled [16] to slotted waveguides with an insertion loss of approximately 8 dB. Optical signal was provided from an Agilent 81680a tunable laser and in some cases an erbium doped fiber amplifier from Keopsys Corporation. A continuous optical signal inserted into a poled polymer ring results in a measurable current established between the two pads, which are electrically connected through a pico-Ammeter. In the most sensitive device, a DC current of ~1.3 nA was observed, indicating an electrical output power of $\sim 10^{-9}$ of the optical input power ($5 \times 10^{-12}$ W of output for approximately .5 mW coupled into the chip). Control devices, in which PMMA or un-poled EO material was substituted, show no photocurrent.

The fact that there is no external bias applied to this system or indeed any energy source, other than the optical signal, demonstrates conclusively that power is being converted from the optical signal. To establish that the conversion mechanism is actually optical rectification, we performed a number of additional experiments. First, we applied a steady bias on the chip for several minutes, as shown in Table 1A, and observed a substantial change in the

#7444 - $15.00 USD Received 16 May, 2005; revised 20 June, 2005; accepted 23 June, 2005

photoresponse of the device. This change depends on the polarity of the bias voltage, consistent with the expected influence of repoling of the device in-place at room temperature. Specifically, if the external bias was applied opposing the original poling direction, conversion efficiency generally decreased, while an external bias in the direction of the original poling field increased conversion efficiency.

Table 1. Polling Results. Part A shows the dependence of the steady state observed current after room temperature biasing with various voltage polarities for one devices. The device was originally polled with a –12 V bias, though at 110 C. With one exception, applying a voltage in the direction of the original polling voltage enhances current conversion efficiencies, while applying a voltage against the direction of the polling voltage reduces the current conversion efficiencies. It should be noted that the power coupled on-chip in these experiments was less than 1 mW due to coupler loss. Part B shows the behavior of several different devices immediately after thermal polling or cycling without voltage. Measurements were taken sequentially from top to bottom for a given device. The only anomaly is the third measurement on device 2; this was after significant testing, and the current observed was substantially less than was observed in previous tests on the same device. We suspect that the polymer was degraded by repeated testing in this case.

Part A:

| Action | New Steady State Current (6 dBm input) |
|---|---|
| Initial State | -5.7 pA |
| +10V for 2 minutes | 0 pA |
| -10V for 2 minutes | -7.1 pA |
| +10V for 2 minutes | -4.4 pA |
| +10V for 4 minutes | -6.1 pA |
| +10 V for 4 minutes | -4.5 pA |
| -10 V for 2 minutes | -14.8 pA |

Part B:

| Device | Action | Current Polarity of Optical Rectification |
|---|---|---|
| 1 | Positive Poling | Positive |
| 1 | Thermal Cycling to poling temperature with no voltage | Rapid fluctuation, did not settle |
| 1 | Negative Poling | Negative |
| 2 | Negative Poling | Negative |
| 2 | Thermal Cycling to Poling temperature with no voltage | None observable |
| 2 | Positive Poling | Negative |
| 3 | Negative Poling | Negative |
| 4 | Positive Poling | Positive |
| 5 | Negative Poling | Negative |

To further understand the photo-conversion mechanism, 5 EO detection devices were poled with both positive and negative polarities, thus reversing the direction of the relative $\chi^2$ tensors. For these materials, the direction $\chi^2$ is known to align with the polling E field direction [12] [18], and we have verified this through Pockels' effect measurements. In all but one case, we observe that the polarity of the generated potential is the same as that used in poling, and the +V terminal during poling acts as the –V terminal in spontaneous current generation, as shown in Table 1B. Furthermore, the polarity of the current is consistent with a virtual voltage source induced through optical rectification. It should be noted that these devices decay significantly over the course of testing, and that in one case the polarity of the

#7444 - $15.00 USD Received 16 May, 2005; revised 20 June, 2005; accepted 23 June, 2005

output current was even observed to spontaneously switch after extensive testing. However, their initial behavior after polling seems largely correlated to the $\chi^2$ direction.

A number of experiments were performed to produce negative results, and to exclude the possibility of a mistaken measurement of photocurrent. The power input to the chip was turned on and off by simply moving the fiber array away from the chip mechanically, without changing the circuit electrically, and the expected change in the electrical output signal of our detector was observed. A chip was coated in polymethylmethacrylate and tested, resulting in no observed photocurrents. Also, we tested some of the devices shown in Table 1 before any polling had been performed; no current was observed.

To establish a quantitative relationship between the laser power in the EO material and the photo-current, we used a lock-in amplifier, and achieved a noise floor of about 0.2 pA. This resulted in a reasonable dynamic range for the 10-200 pA photocurrent readings. Figure 3(a) and 3(b) show optical transmission curves for typical devices. Figure 3(c) shows several traces of output current versus input laser power, and a fairly linear relationship is observed. The relationship $I = cP$, where I is the output current, P is the input laser power, and c is a proportionality constant ranging from 88 +/- 10 pA/mW at a 1 kHz lock-in measurement and when the wavelength is on resonance, changing to a lower value of 58+/-8 pA/mW off resonance for our best device. It is important to note that current was easily observed with only a pico-ammeter, or by simply connecting an oscilloscope to the output terminal and observing the voltage deflection.

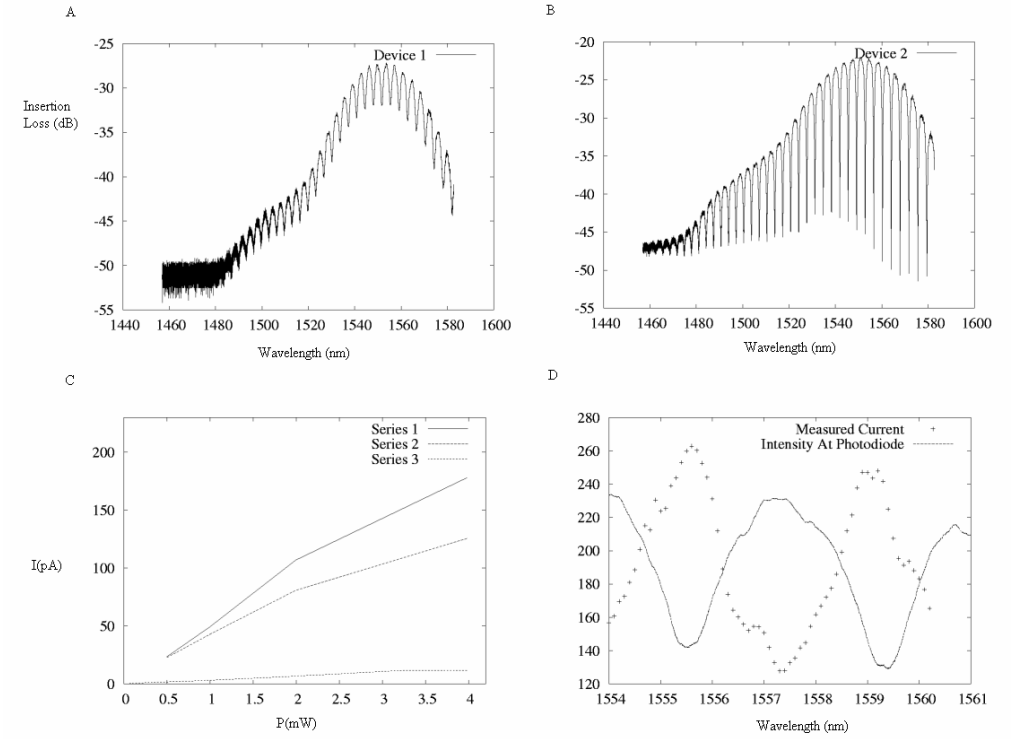


Fig. 3. Panel A shows the transmission spectrum of detector device 1, whereas B shows detector device 2. Panel C shows several curves of current vs. power for three measurement series. Series 1 is of the first device with the wavelength at1549.26 nm, on a resonance peak. Series 2 is the first device with the wavelength at 1550.5 nm off resonance. Series 3 is for device 2, with the wavelength at 1551.3, on resonance. Finally, panel D shows the output current as a function of wavelength, overlaid with the transmission spectrum. The transmission spectrum has been arbitrarily rescaled to show the contrast.

#7444 - $15.00 USD Received 16 May, 2005; revised 20 June, 2005; accepted 23 June, 2005

As another demonstration of the dependence of the output current on the amount of light coupled into the resonator, we also tuned the laser frequency and measured the output current. As can be seen in Fig. 3(D), the amount of output current increases as the laser is tuned onto a resonance peak. This again indicates that the overlap between the EO polymer in the resonator and the optical mode is responsible for the photo-current. We have overlaid a photocurrent vs. wavelength response scan to show the resonance peaks for comparison. It should not be surprising that a small photocurrent is still measured when the laser is off resonance, since the amount of radiation in a low-Q ring resonator is non-negligible even off resonance. It is also worth noting that we have successfully observed this detector function at speeds up to 1 MHz, without significant observable rolloff. This is again consistent with optical rectification. Unfortunately, our devices could not be measured at higher speeds, due to substantial output impedance.

The conversion efficiency from our first experiments is certainly several orders of magnitude below the ultimate limit, and can be explained by the high insertion losses in our system. 75% of the input power in the fiber is not coupled onto the chip and our low-Q resonators only provide a limited path length within which light can interact with the electrooptic material. Furthermore, by design a great deal of the light in the resonator will be dumped to an output port, and not absorbed. It is expected that with further design and higher-Q resonators, the efficiency of these devices can be greatly increased. It is, however, important to note that nothing about this effect depends on the presence of rings. The rings provide a convenient and compact device for observing these effects, but one could just as easily observe optical rectification by using a long, polymer coated, split waveguide, with each side connected to an electrical pad.

*3.2 Pockels' effect modulation*

At DC, the Pockels effect was measured by applying varying voltages to the device and observing the device transmission as a function of wavelength. For devices with working modulation, the resonance peaks were shifted, often to a noticeable degree. To counter the systemic drift due to temperature fluctuations, a series of random voltages were applied to a device under test and the wavelength responses noted. The intersection of a resonance peak and a certain extinction, chosen to be at least 10 dB above the noise floor, was followed across multiple scans. A 2d linear regression was performed, resulting in two coefficients, one relating drift to time, and one relating drift to voltage.

At AC, a square wave input voltage was put across the device. The input wavelength was tuned until the output signal had the maximum extinction. It was determined what power levels were implied by the output voltage, and then the observed power levels were fit to a wavelength sweep of the resonance peak. This readily allowed the tuning range to be calculated. We successfully measured AC tuning up to the low MHz regime; the limitation at this speed was noise in our electrical driving signal path, not, as far as we can tell, any rolloff in the modulation process itself.

In Fig. 4, a result at approximately 6 MHz for the use of these structures as resonantly enhanced electro-optic modulators is shown. These experiments clearly demonstrate that low-voltage electro-optic tuning and modulation can be achieved in the same geometries as have been described for photodetection. It should be emphasized that these devices are not optimized as modulators. By increasing the Q of the resonators to exceed 20,000, which has been demonstrated elsewhere [6], it will be possible to achieve much larger extinction values per applied voltage.

By utilizing new dendrimer-based electrooptic materials [14], we have achieved .042±.008 nm/V, or 5.2±1 GHz/V for these rings. This implies an $r_{33}$ of 79±15 pm/V. This result is better than those obtained [12] for rings of 750 micron radius, which we believe to be the best tuning figure published to date. By contrast, our rings have radii of 40 microns. We credit our improvement over the previous results mainly to the field enhancement properties of our waveguide geometry.

#7444 - $15.00 USD Received 16 May, 2005; revised 20 June, 2005; accepted 23 June, 2005

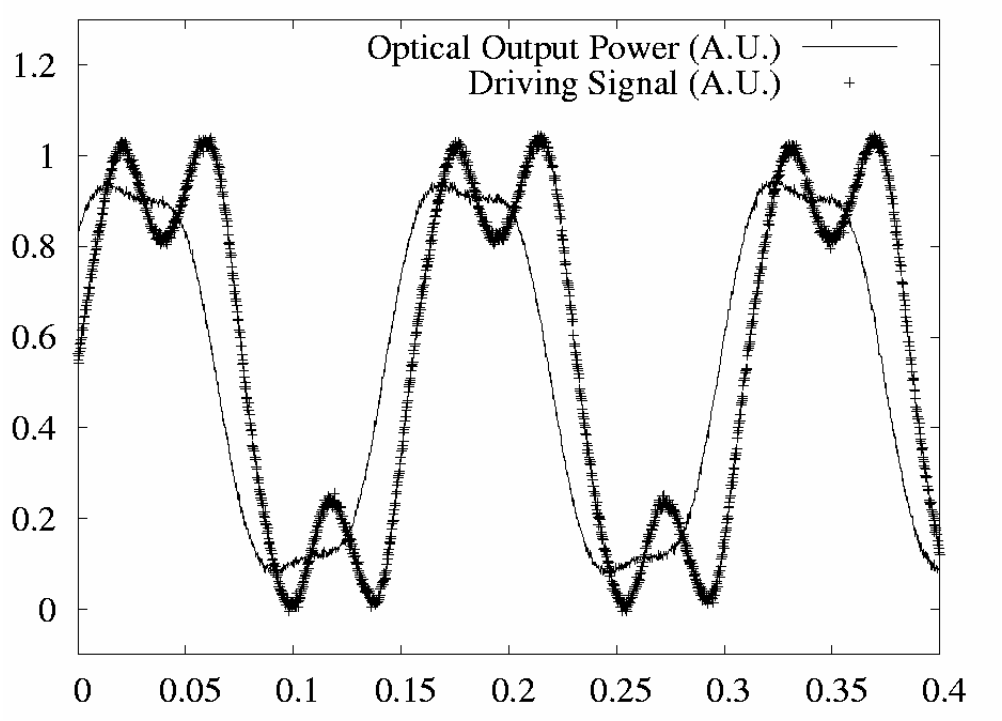


Fig. 4. Bit pattern generated by Pockels' Effect modulation 5 dB. The vertical axis represents input voltage and output power, both in arbitrary units. Horizontal axis is time in microseconds. Voltage swing is on the input signal is 20 volts.

**4. Analysis**

*4.1 Optical rectification theory*

The general governing equation of nonlinear optics is known [17] to be:

$$D_i = \varepsilon_0(\varepsilon_r E_i + \chi_{ijk}{}^2 E_j E_k + ...) \tag{1}$$

Our EO polymers are designed to exhibit a relatively strong $\chi^2$ moment, ranging from 10-100 pm/V. In most $\chi^2$ EO polymer systems, the Pockel's effect is used to allow the electric field (due to a DC or RF modulation signal) to modify the index of refraction. In such systems the modulating electric field is typically far in excess of the electric field from the optical signal and the term that produces the material birefringence is the only term of importance in the above equation.

Our waveguides, however, have a very large electric field as most of the radiation is confined to a 0.01 square micron cross section. It can be shown that the electric field is approximately uniform in the transverse direction, with a magnitude of

$$10^8 \sqrt{P} \frac{V}{m} \tag{2}$$

where P is the optical power in Watts. At large optical fields, the non-Pockels terms involved in the governing nonlinear equation cannot be neglected. For coherent input power, at a given location in the waveguide, the optical field is:

#7444 - $15.00 USD Received 16 May, 2005; revised 20 June, 2005; accepted 23 June, 2005

$$E_{optical}(t) = A\cos(wt + \theta) \tag{3}$$

The term

$$E_{optical}{}^{2} = \frac{A^2}{2}\cos(2(wt + \theta)) + \frac{A^2}{2} \tag{4}$$

will therefore contain not only frequency doubled components, but also a "DC" component. This phenomenon is known as optical rectification [18]. We believe that this DC component provides a likely explanation for the photo-current that we observe. Because we have positioned electrodes (the two sides of the slot waveguide) at precisely the bounds of the induced field, the effect of optical rectification takes a small slice of the optical power and converts it into a virtual voltage source between the two arms. This in turn induces a current that we can measure and is linearly proportional to the input power $E_{optical}{}^{2}$.

Now let us consider the solution to Maxwell's equation in more detail. Our system can be approximated for this discussion as having two dimensions, with both the optical and DC electric field in the x direction and propagation in the z direction, for instance. Let us imagine that the $\chi^2$ is nonzero and small for a tiny region from 0 to w in the x dimension. $\chi^2$ is sufficiently small that the electric field due to the optical mode is still uniform. Let us imagine the system has no charge anywhere. The optical electric field can be written as $E = Ae^{ikz-iwt} + c.c.$ where c.c. indicates a complex conjugate. Let us further assume that the rectified DC field is of real amplitude C and uniformly directed in the x dimension on (0, w), and 0 elsewhere.

Other than the divergence condition, Maxwell's equations are still satisfied by this system. But at the edge of an interface on the interior, the DC frequency component of $D_x$, the displacement electric field, is discontinuous. At x=0, we have:

$$D_x{}^{-} = 0 \tag{5}$$

$$D_x{}^{+} = \varepsilon_0(\varepsilon_r C + \chi^2 C^2 + 2\chi^2 \mid A \mid^2) \tag{6}$$

We neglect $\chi^2$ C2 because we expect the amplitude of the rectified field to be far smaller than that of the optical field. Clearly, the boundary condition of zero divergence can only be satisfied if Dx+ is 0. Then,

$$C = -\frac{2\chi^2}{\varepsilon_r} \mid A \mid^2 \tag{7}$$

So we see that the direction of the rectified field is reversed compared to the direction of $\chi^2$. Note that there is no particular direction associated with the optical field as it is continually oscillating. As we have seen, this rectified DC field would then, if acting as a virtual voltage source, create an effective positive terminal on the positive polling terminal.

*4.2 Analysis of data for optical rectification*

To derive the magnitude of the expected photocurrent, we assume that the $\chi^2$ magnitude relating to the Pockels' effect is similar to that for optical rectification. A measurement of $\chi^2$ can then be obtained from the direct observation of the electro-optic coefficient by the standard measurements described earlier. The typical measured tuning value of 2GHz/V yields approximately 50 pm/V.

#7444 - $15.00 USD Received 16 May, 2005; revised 20 June, 2005; accepted 23 June, 2005

In the best case, devices with 6 dBm of input power returned approximately 1.4 nA of current. With Qs ranging from 3k to 5k, and assuming approximately 7 dB of insertion loss in the input grating coupler on one of our chips, in the best case as much as 0 dBm might be circulating in a resonator on resonance. This implies a peak electric field due to the optical signal of approximately $3.1 \times 10^6$ V/m. The induced static nonlinear polarization field is then nearly 1000 V/m, which amounts to a voltage drop of $14 \times 10^{-5}$ V across a 140 nm gap. If this voltage is assumed to be perfectly maintained, and the load resistance is assumed to be 5 MΩ, then 28 pA would be generated, about a factor of 100 less than is observed in the largest measurement made, but within a factor of 20 of the typical measurement of 352 pA for 6 dBm of input. Significantly, because the generated current is quadratic in E, it is clear that the current will be linearly proportional to the input intensity. This is in accordance with our observations. The best results for optical rectification were obtained with YLD/APC polymer, wheras our best Pockels' Effect results were obtained with the dendrimer materials.

Significantly, the sign of the output current matches that which would be predicted by nonlinear optical rectification, as predicted in section 4.1. Specifically, since positive current emanates from the positive terminal, the rectified E field has a sign reversed from the $\chi^2$ and the polling E field. It should be noted that it is a well established fact with these materials that the $\chi^2$ direction tends to align with the direction of the polling E field. Because of this, the rectified field acting as a voltage source will produce an effective positive terminal at the terminal that had the positive polling voltage.

We do not yet fully understand the current generation mechanism. In particular, it is not clear what provides the mechanism for charge transport across the gap. The APC material in which the nonlinear polymer is hosted is insulating, and though it does exhibit the photoconductivity effect due to visible light, it is unclear whether it can for near-infrared radiation. Photoconductivity due to second harmonic generation may play a role in this effect. It is certainly the case, however, that current flows through this gap; that is the only region in the entire system where an electromotive force exists. Also, photoconductivity alone is not adequate to explain the reversal of the current coming off of the detector devices when the poling direction is reversed, nor the conversion of the optical input into directed current in general. The only mechanism to our knowledge that adequately explains this data is optical rectification.

If we assume that it will be possible to achieve a 10x improvement in the Q's of the resonators, while still getting more than 10 dB of extinction, then the intensity circulating in such a ring would be about 13 dB up from the intensity of the input wave. By comparison, with a Q of about 1000 and high extinction, the peak circulating intensity is about the same as the intensity in the input waveguide. So it's reasonable to expect that it will be possible to get at least 10 dB of improvement in the circulating intensity, and thus in the conversion efficiency, by fabricating higher Q rings.

Because the optical losses of the polymer and dendrimer materials could turn out to be a limiting factor for the performance of higher-Q devices, a thorough study of the optical losses of these materials is needed. Because the devices used herein were deliberately designed to have low Q's, they are not the ideal system for examining such losses. It is possible to say that an upper bound of about 10dB/cm of loss is reasonable, based on our observations that the Q's of the resonators did not change dramatically after being coated with the organic materials. However, further work is clearly required to determine whether the optical loss in these materials will prove to be a limiting factor in device performance.

## 5. Conclusion

By means of our nano-scale slotted waveguide geometry, we have obtained massive enhancement of the optical field. That has in turn enabled us to exploit nonlinear optical processes that are typically only available in the kW regime in the sub-mW regime. This difference is so considerable that we believe it represents a change in kind for the function of nonlinear optical devices; it may be possible to someday construct a practical, low-power

#7444 - $15.00 USD Received 16 May, 2005; revised 20 June, 2005; accepted 23 June, 2005

detector based on nonlinear optical rectification. In addition, we expect this hybrid material system to provide a means for creating compact devices that exploit other nonlinear phenomena on-chip.

Optical rectification based detectors might have many advantages over currently available technology. In particular, such detectors would probably be able to function at a higher intrinsic rate than the typical photodiode in use, as the optical rectification process occurs at the optical frequency itself, on the order of 100 THz in WDM systems. The absence of an external bias, and the generation of a voltage rather than a change in current flow, might also prove easier to handle electronically. We also do not believe that a device based on nonlinear optical rectification would suffer from the limitation of a dark current. This in turn might mean that current WDM systems could function with lower optical power, providing numerous benefits. Similarly, our demonstration of enhanced modulation using these waveguide geometries may also lead to useful components in future communications systems.

We conclude by stressing the economic aspects of our development. Because our devices can be fabricated in planar, electronics grade silicon-on-Insulator, using processes compatible with advanced CMOS processing, it is likely the devices based on these principles could be built cheaply. It is our hope that electrically active slotted waveguides can someday become a platform of choice for practical linear and nonlinear integrated optics.

**Acknowledgments**

The authors are thankful for many fruitful discussions with Hal Hagar and Bill Krug of the Boeing Corporation and gratefully acknowledge DARPA and NAVAIR for support under N00421-02-D-3223.

#7444 - $15.00 USD Received 16 May, 2005; revised 20 June, 2005; accepted 23 June, 2005